in *Transport versus Structure in Biophysics and Chemistry*,
S.C. Müller, J. Parisi, W. Zimmermann (Eds.),
Lecture Notes in Physics, (Springer-Verlag, Berlin 1999).

~~in Druck~~

Pattern formation in the developing visual cortex

Siegrid Löwel[1] and Fred Wolf[2]

[1] Leibniz-Institut für Neurobiologie,
Forschergruppe 'Visuelle Entwicklung und Plastizität'
Brenneckestr. 6, D-39118 Magdeburg, Germany
[2] Max-Planck-Institut für Strömungsforschung,
Abteilung Nichtlineare Dynamik,
Bunsenstr. 10, D-37073 Göttingen, Germany

Abstract. In the visual cortex of the brain, neurons specialized to process particular aspects of the visual input are arranged in complex spatial patterns, called cortical maps, and interact through a dense network of intracortical connections. Many experimental results are consistent with the hypothesis that the precise organization of patterns and connections within the cortex is not predetermined by genetic instructions, but emerges through activity-dependent self-organization during the first months of life. In this chapter, we will first survey the layout of visual cortical maps and the structure of intracortical connections, and then discuss their activity-dependent development. In the subsequent sections of the chapter, we will discuss the formation of patterns in the developing visual cortex from a nonlinear dynamics perspective. In particular, we will analyze the instability mechanisms, through which cortical patterns presumably emerge early in development. We will also discuss the intriguing possibility that cortical patterns undergo substantial rearrangement during the first months of life.

1 Experimental observations

1.1 Maps and connectivity patterns in the visual cortex

In all mammals including man, visual information from the retina is relayed via a thalamic nucleus to the primary visual cortex at the occipital pole of the brain (Fig. 1) (for a general introduction to visual information processing see [1]). From the many visual cortical areas that have been described to date we will focus in this chapter on the largest individual area, namely the primary visual cortex, also termed area 17 in the terminology of the anatomist Korbinius Brodmann who divided the human cortex according to cytoarchitectonic criteria and consecutively numbered all identified areas. In cats, area 17 is about $380mm^2$ in size and consists - like other cortical areas - of six layers of nerve cells (layers I-VI) extending over about 2 mm from the pial surface of the brain down to the white matter, a region containing axons entering the cortex, as well as those leaving it.

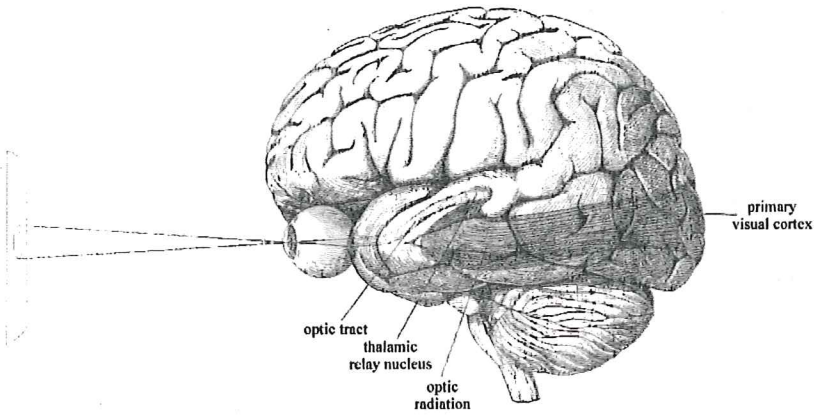

Fig. 1. The major flow of visual information in the brain: The ganglion cells of the retina send their axons (via optic nerve and optic tract) to a thalamic relay nucleus that in turn projects (via the optic radiation) to the primary visual cortex at the occipital pole of the brain[1].

While retinal ganglion cells have concentric receptive fields and can be activated by spots of light, neurons at higher levels of the visual pathway become increasingly selective in their stimulus requirements. For example, neurons in area 17 respond to light-dark edges only if they are presented at a certain orientation. This property is called 'orientation selectivity'. Similarly, neurons very often are more strongly driven by visual stimulation of one eye compared to the other. This property is termed their 'ocular dominance'. In addition, neurons are selective for a variety of other stimulus parameters including the direction of a moving contour or a particular spatial frequency or disparity of the stimulus [3]. Interestingly, neurons that respond to similar visual stimuli, e.g. to lines of a particular orientation presented at a particular location in the visual field (within their receptive field), are not distributed randomly across the cortex but are arranged in columns extending from layer I to layer IV (in this case, the so-called 'orientation columns' [4, 2]). In a plane parallel to the cortical surface, neuronal selectivites vary systematically so that columns of similar orientation or eye preference form highly organized periodic patterns. The anatomical basis of the ocular dominance columns are the thalamocortical afferents of the two eyes that terminate in separate domains in the input layer IV of the visual cortex. Thus neurons in these segregated domains (ocular dominance domains) get preferential input

[1] Adapted from: EYE,BRAIN, AND VISION by Hubel[2] ©1988 by Scientific American Library. Used with permission by W.H.Freeman and Company.

from one eye only and are therefore dominated by visual stimulation of that particular eye. In analogy, the receptive fields of the thalamocortical afferents to single orientation columns are elongated in visual space in a direction that parallels the preferred orientation of the recipient cortical cells. This geometrical alignment is however not the sole basis of simple cell orientation selectivity since both excitatory and inhibitory intracortical connections have been shown to influence this functional property (for a recent review see [5]).

Cortical neurons interact through a dense network of intracortical connections. The classical view of connections within the cortex is that axons run predominantly in a direction perpendicular to the cortical surface, from layer to layer, with relatively little spread in a direction parallel to the cortical surface. However more recent experiments have clearly established that extensive horizontal connections do span several millimeters (up to 8mm) within individual cortical layers [6]. These connections are termed long-range horizontal, or tangential. Their synapses exhibit the morphology of excitatory synapses and contact excitatory and inhibitory neurons in the proportion with which these cell types occur in the cortex. Long-range connections got particularly prominent in recent years because they span a cortical region much larger than that corresponding to the classical receptive field of an individual neuron which allows them to integrate information from widely distant points in the visual field. The long-range fibers are not distributed homogeneously across the cortex but terminate in discrete clusters thus interconnecting regularly spaced groups of neurons. Evidence has accumulated in the last years showing that interconnected cell groups share similar functional properties (Fig. 2) (for review see [7]).

In the past, functional maps have been visualized with a variety of techniques that allow to portray the activity of a large number of neurons (e.g. radioactive staining for functional activity [8]). Over the last decade, with the advent of new minimal-invasive imaging techniques it has become possible to directly visualize cortical activity patterns with unprecedented accuracy and to follow up their possible experience-dependent changes with time. The so-called 'optical imaging of intrinsic signals' exploits the fact that active cortical regions absorb more light of a certain wavelength (dark red light between $605 - 750nm$) compared to inactive regions. Therefore active regions appear darker on images taken from the exposed cortex compared to inactive ones. The activity-dependent component of the absorbance changes is however only one promille in size compared to the entire signal [9] (for review see [10]).

Using optical imaging of intrinsic signals, Bonhoeffer and Grinvald visualized the layout of cat area 18 for the first time with high spatial resolution ([11]; see also [12]). They confirmed the clustering of neurons with similar response properties and observed that iso-orientation domains were arranged radially, in a pinwheel-like fashion, around singularites. In all pinwheels, orientation preference changed either clockwise or counterclockwise

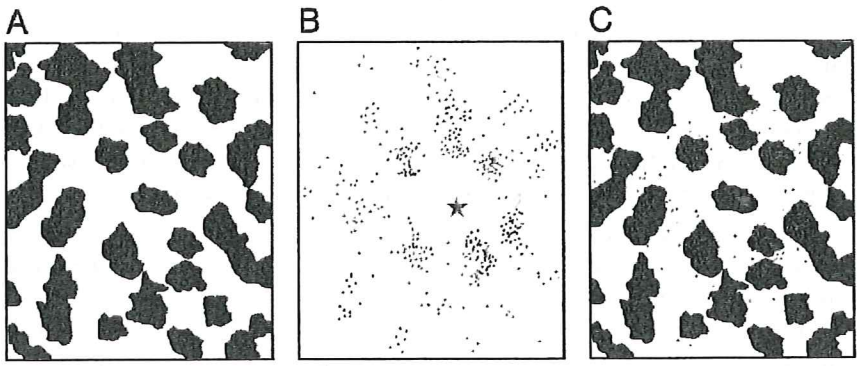

Fig. 2. Columnar specificity of long-range tangential connections. Schematic drawing of the topographic relationship between long-range connections and orientation columns in the primary visual cortex of cats. A: Pattern of orientation columns (black regions represent cortical regions activated by horizontal moving contours). B: After an injection of a neuronal tracer in the same region of cortex, labelled neurons (marked by dots) have a patchy distribution. C: Superposition of A and B. Note that the injection site of the neuronal tracer (marked with an asterisk) was located in a black column (i.e. a horizontal orientation column) and that labelled neurons are predominantly but not exclusively distributed within columns of the same functional preference (other dark columns). Modified from [7].

and all orientations appeared only once per pinwheel-center (Fig. 5A). Orientation preference maps exhibiting a similar organization have been observed in a variety of species [13, 14, 15, 16, 17, 18, 19].

1.2 Developmental plasticity of cortical patterns

One of the most fascinating questions in developmental neurobiology is how these maps or in general cortical functional architecture develop and whether experience and neuronal activity play an important role or not. One way to approach these questions is to analyze the brains of animals that were raised with modified sensory experience. Possible changes in functional achitecture compared to normally raised controls demonstrate the importance of experience for normal brain development. According to Hebb's postulate for associative learning [20] the connection strength between two nerve cells is not fixed but can be modified by a correlation-based mechanism: synaptic contacts between synchronously active pre- and postsynaptic neurons are selectively strengthened whereas synaptic contacts between asynchronously active pre- and postsynaptic neurons will be weakened. Correlation-based mechansims inspired by Hebb's original ideas about the modification of synapses have been proposed to explain a variety of phenomena including the development

of ocular dominance columns [21, 22, 23] and orientation columns [24, 25] in the visual cortex. One particular fruitful experimental model - not only for the analysis of experience-dependent changes but also for elucidating underlying principles of cortical organization - is the investigation of strabismic animals. In these animals, the optical axes of the two eyes are no longer aligned so that the images on the two retinae cannot be brought into register. As a consequence, the responses mediated by anatomically corresponding retinal loci in the two eyes are no longer correlated. Possible changes in cortical architecture in strabismic animals can therefore be interpreted as resulting from the decorrelation of activity between the two eyes.

In the following, we will present examples of activity-dependent cortical development for three of the patterned cortical systems briefly introduced above: the pattern of cortical functional maps, the pattern of thalamocortical afferents (ocular dominance columns) and the pattern of intracortical connections.

1.2.1 Intracortical connections

When kittens and humans are born, clustered long-range connections are absent. Tangential fibers develop mainly after birth and attain their adult specificity within the first weeks of life [26] (for review see [7]). The emergence of well-segregated clusters of interconnected cells in a developmental period during which visual experience is known to profoundly influence cortical development [27] indicated that the specificity of these connections might also depend on visual experience. In particular, the anatomical observation that clusters refine by the elimination of one set of connections and the stabilization of another set of connections raised the possibility that selective stabilization is influenced by neuronal activity and not genetically determined. Experiments with visually deprived animals confirmed this hypothesis by showing that in binocularly deprived and dark-reared cats, the selectivity of long-range intracortical connections was severly reduced and the normal and selective adult pattern of connectivity did not appear [26]. Direct evidence for the hypothesis that long-range connections are stabilized between cells exhibiting correlated activity was obtained in our experiments with strabismic cats [28]. As briefly mentioned above, the amount of activity reaching the cortex in these animals is normal, however the correlation of activity between the eyes is severely reduced. As a consequence, squint accentuates the segregation of the thalamocortical afferents of the two eyes in layer IV and most of the cells in the visual cortex become responsive to stimulation of either the left or the right eye [2]. Each of these monocularly driven cell populations is capable of subserving normal pattern vision. However, strabismics lose the capability to combine information coming from the two eyes into a single percept.

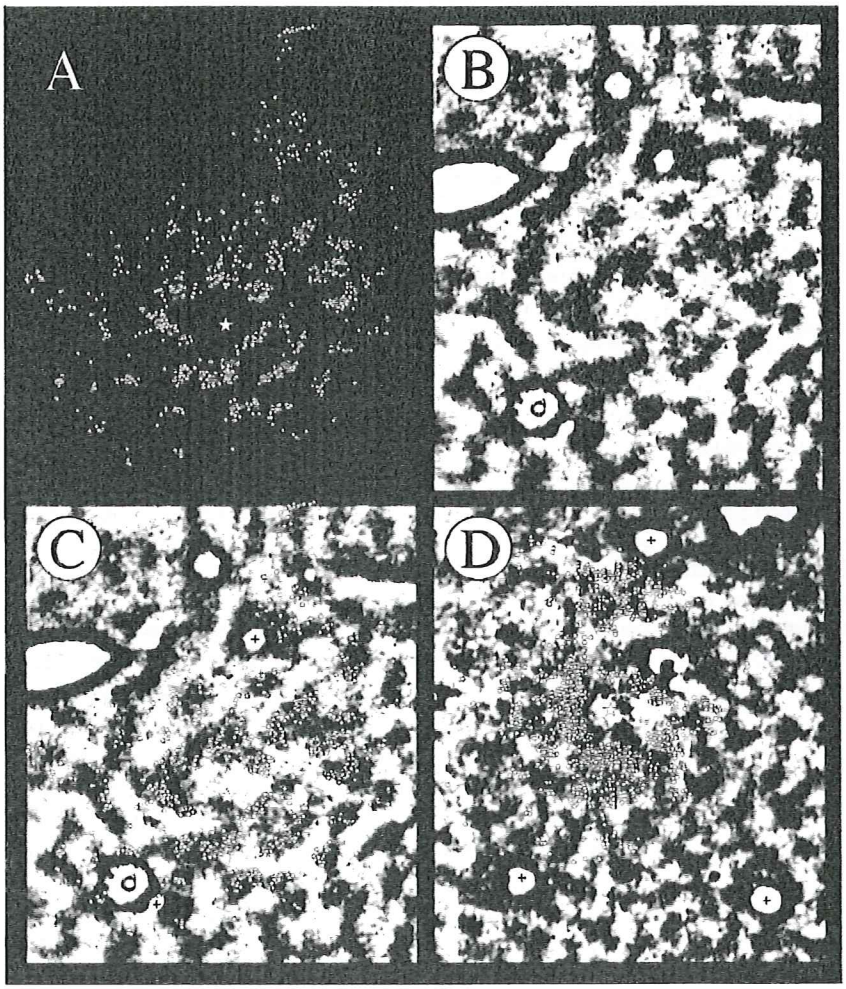

Our experiments revealed that in area 17 of divergently squinting cats cell clusters were almost exclusively driven from either the left or the right eye and tangential intracortical fibers preferentially connected cell groups activated by the same eye [28]. After injections of neuronal tracers into the primary visual cortex, labelled neurons were distributed in well-segregated clusters up to 5 mm from the injection site. The locations of cell groups preferentially activated by either the right or the left eye (ocular dominance columns) were visualized with a radioactive staining protocol for functional activity, the so-called [14C]2-deoxyglucose (2-DG) method [29]: after monocular visual stimulation, regions of increased neuronal activity take up more

Fig. 3. Experience-dependent selection of long-range intracortical connections. Topographic relations between ocular dominance columns and long-range connections in the primary visual cortex of a strabismic (A-C) and a normally raised cat (D). A: Distribution of labelled cells after an injection with a fluorescent neuronal tracer. White dots, the position of individual cells; asterisk, injection site. B: 2-deoxyglucose pattern showing the topography of ocular dominance territories in the region containing the labelled cells in (A). The black regions represent the domains of the right eye. C: Superposition of (A) and (B). Most of the labelled cells are located within zones of high 2-DG up take (black regions). The injection site was located in a right eye domain. D: Superposition of ocular dominance domains (black regions) and labelled neurons (white dots) in a normally raised cat. Note the absence of a systematic topographic relationship between the two patterns. Modified from [7].

of the radioactively labelled glucose analogue than less active regions, accumulate the radioligand and thus can be visualized autoradiographically by exposing brain sections to X-ray film. The X-ray films get dark in regions of increased radioactivity and thus in regions of increased neuronal activity. Comparison of the patterns of labelled neurons with the 2-DG labelled ocular dominance columns revealed that cell clusters were located preferentially within the same ocular dominance territories as the injection site (Fig. 3). Analyses of normally reared control animals provided no evidence for an eye-specific selectivity of tangential connections. This agreed with other evidence that in normally reared cats, tangential connections are related to orientation but not to ocular dominance columns [30, 31]. These results suggested that the development of long-range intracortical connections depended on experience-dependent selection mechanisms similar to those in the development of thalamocortical connections [27]: 'neurons wire together if they fire together' [28].

Extending these experiments we could further show that i) callosal connections (connections linking the two hemispheres of the brain that guarantee a continuous representation of the left and right visual field) also extend predominantly between neurons activated by the same eye and preferring similar orientations and ii) that tangential connections remain confined to columns of similar orientations within the subsystems of left and right eye domains [31]. Thus the selection mechanisms for the stabilization of callosal connections are similar to those that are responsible for the specification of the tangential intracortical connections and strabismus does not interfere with the tendency of long-range horizontal fibers to predominantly link neurons of similar orientation preference.

These anatomical results are compatible with the idea of a selective stabilization of tangential fibers between coactive groups of neurons. They support the hypothesis that the strength of long-range connections in the primary visual cortex reflects the frequency of previous correlated activation.

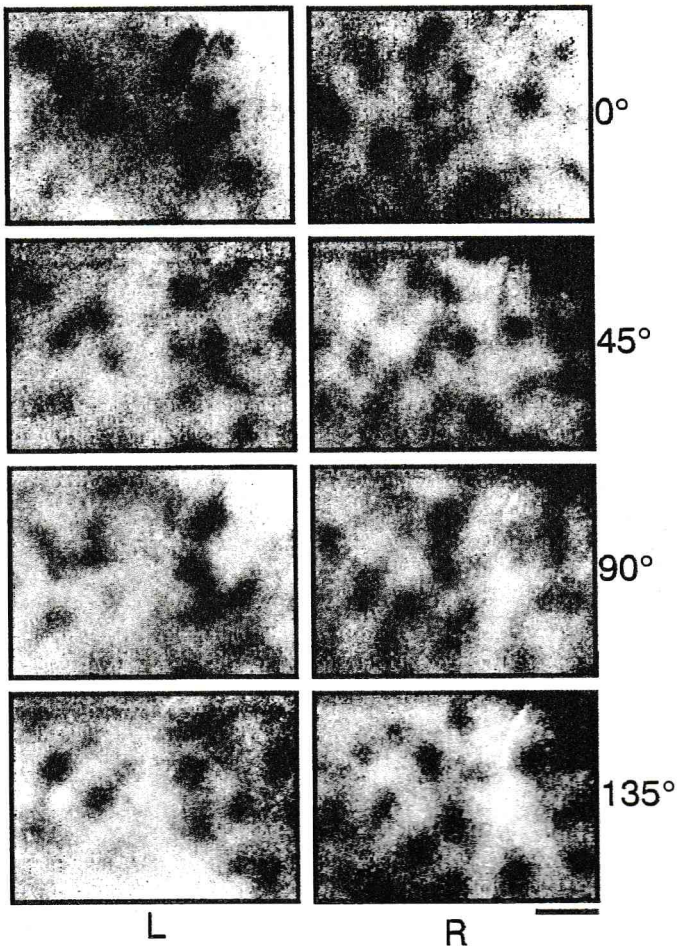

Fig. 4. Monocular orientation domains in the left area 17 of a strabismic cat. The imaged cortical region is about 4.8 x 3.6 mm in size. Cortical activation patterns visualized by optical imaging of intrinsic signals while the animal was stimulated through the left (L, left column) and right eye (R, right column) with oriented gratings of 0^o, 45^o, 90^o and 135^o (from top to bottom). Note that the patterns are clearly different for left and right eye stimulation. Modified from [32].

1.2.2 Functional maps

In the primary visual cortex of cats, the elimination of correlated activity between the two eyes enhances the segregation of the thalamocortical afferents into alternating ocular dominance columns [2]. In addition, both tangential

intracortical connections and neuronal synchronization are severely reduced between neurons activated by different eyes [32]. Thus, the sets of ocular dominance columns related to different eyes are rather independent of each other raising the question whether this affects the organization of iso-orientation domains. If visually correlated activity plays a similarly important role for the development of orientation columns as it does for the development of long-range tangential fibers, then iso-orientation domains activated by different eyes should distribute independently, i.e. they should not be continuous across the boundaries between different ocular dominance domains. To examine this question, we visualized the layout of iso-orientation and ocular dominance columns in area 17 of strabismic and normally raised cats using both conventional mapping techniques and optical imaging of intrinsic signals [32]. In Figure 4, examples of monocular orientation domains in area 17 of one strabismic animal are shown. Dark patches correspond to activated cortical regions, light grey patches were not activated above threshold. The recorded maps were about 3.6x4.8mm^2 in size. The great advantage of the imaging technique, not previously achieved with comparable spatial resolution with any other mapping technique, is the ability to compare activity patterns from the same cortical region repeatedly using a library of different stimuli. In the illustrated case, the animal was stimulated with moving gratings of four different orientations through either the left or the right eye. The activity patterns consisted of rather isolated patches and - as expected for strabismic animals - were different after activation through the right and left eye.

Thus ocular dominance columns can readily be visualized with optical recording (Fig. 5) (in contrast, in normally raised animals, the visualization of ocular dominance columns becomes increasingly difficult after a few weeks of life because maps induced through the two eyes become nearly identical [33]): Regions activated by the left eye (dark regions in Figure 5B) appear almost inactive with stimulation of the right eye (white regions in C) and vice versa (Fig. 5B,C). To analyze the geometrical relationship between iso-orientation domains and ocular dominance columns, orientation preference maps were computed by vectorial summation of the responses to the different stimulus conditions. In these angle maps, a color-code is used to display the orientation that elicited the maximal response at a particualar cortical region. In all our strabismic cats, the angle-maps displayed a pinwheel-like organization of iso-orientation domains (Fig. 5A,D) - as described previously for normally raised macaque monkeys, cats, ferrets and tree shrews [13, 14, 15, 16, 17, 18, 19].

Comparing orientation with ocular dominance maps revealed that iso-orientation domains were continuous across the borders of ocular dominance columns (Fig. 5E). To analyze this continuity quantitatively, we determined the angle of intersection between orientation and ocular dominance columns. Iso-orientation contours tended to cross the borders between ocular dominance columns at steep angles. Figure 6 shows histograms of intersection

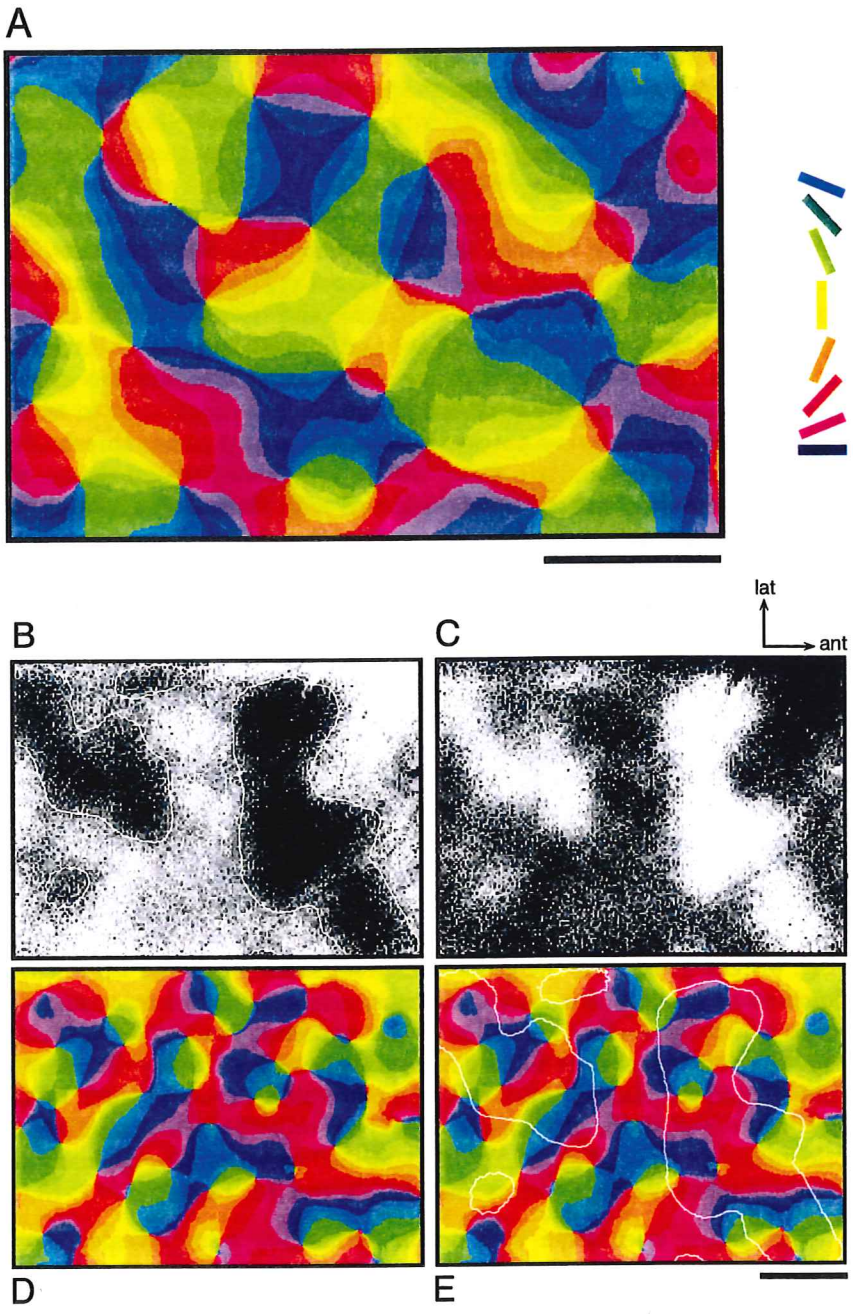
A
B
C
lat
ant
D
E

angles in 3 strabismic cats, revealing a strong preponderance of angles between 75 and 90 degrees. A similar distribution of intersection angles has been described in V1 of macaque monkeys and area 17 of normally raised cats [14, 35, 36, 37]. Thus there is a systematic geometrical relationship between the two columnar systems as originally suggested by Hubel and Wiesel [38] on the basis of electrophysiological studies. This arrangement is well adapted because it permits the coverage of a particular point in the visual field with all relevant combinations of orientation preference and ocular dominance in the smallest possible volume of cortex [39].

The major finding of our imaging studies is that in strabismic cats, iso-orientation domains remain continuous across the borders of ocular dominance columns [32]. The observation is remarkable in view of the nearly complete structural and functional segregation of these columns in strabismic animals. The most likely explanation for this observation is that in cat area 17 the basic layout of orientation preference maps is specified before the age at which we had induced strabismus and that the subsequent rearrangement of thalamic input and of tangential intracortical connections occurred within the scaffold of the already fixed map of orientation preferences. This possibility is supported by several observations. First, orientation selective neurons can be found already in visually inexperienced kittens before eye opening [40]. Second, the maturation of orientation selective neurons is rather independent of visual experience until three weeks of age [33]. Third, iso-orientation maps remain unchanged even if thalamocortical input connections get rearranged as a consequence of manipulated visual experience [41, 42, 43]. This does not imply that neuronal activity plays no role in organizing orientation maps. The role of spontaneous activity patterns for the initial development of cortical

Fig. 5. Functional maps in area 17 of strabismic cats. (A) Orientation preference ('angle') map in a 4.1 mm x 2.8 mm large region of the primary visual cortex. The preferred orientation for every region of the imaged cortex is color-coded according to the scheme on the right side of the figure. Note the pinwheel-like organization of orientation domains: there are numerous singularities in the map around which all colors (orientations) appear once. (B-E) Segregated ocular dominance domains and orientation preference maps in area 17 of another animal. (B, C) Activation patterns for the left (B) and right eye (C) are complemetary: Regions heavily activated by the left eye (dark regions in B, outlined in white) are only weakly activated by the right eye (light grey regions in C). Note that the domains of the left, ipsilateral eye appear as dark islands on a light grey sea. (D) Orientation preference ('angle') map of the same piece of cortex as in B and C. (E) Topographic relationship between iso-orientation domains and ocular dominance columns. Superposition of the angle map (D) and the outlined borders of adjacent ocular dominance columns (white contours in B). Note that domains of like orientation preference labelled by the same color in the angle map are continuous across the borders of adjacent ocular dominance domains. Scale bars 1 mm. Modified from [32].

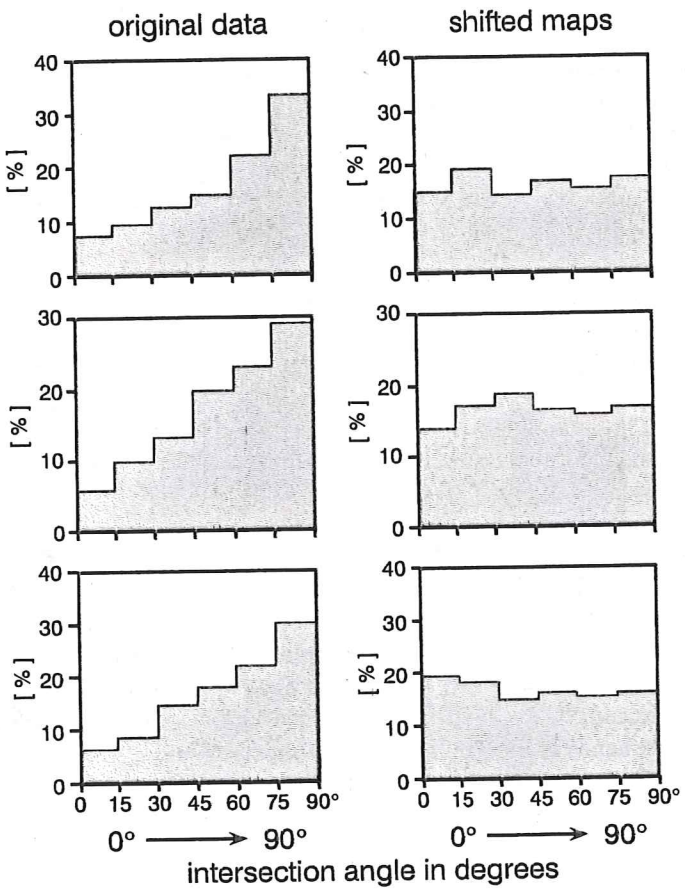

Fig. 6. Histograms of intersection angles between iso-orientation and ocular dominance columns in three strabismic cats. x-axis, intersection angle in degrees from 0^o to 90^o, divided into six classes ($0^o - 15^o$, $15^o - 30^o$, ...). y-axis, percentage of intersection angles in the respective class. Left column, original data. Right column, *shiftet* maps: iso-orientation contours of one animal superimposed with the ocular dominance borders of another animal. Note that intersection angles between 75^o and 90^o are most abundant in the original data of all cases. Note in addition that the histograms are always flat after shifting the maps. Modified from [32].

maps is a highly debated issue at the moment. Spontaneous activity waves of both cortical and thalamic origin have been described and might determine the layout of orientation maps and the early experience-independent clustering of tangential connections.

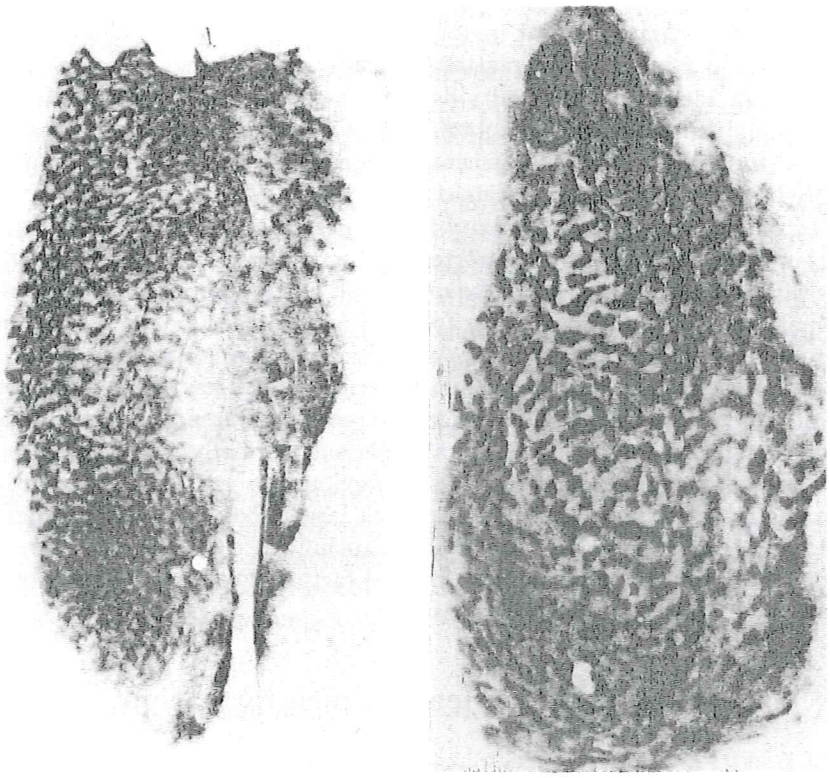

Fig. 7. Overall pattern of ocular dominance columns in area 17 of a strabismic (right) and a normally raised cat (left). The characteristic wavelength of the right pattern is larger than that of the left pattern. Modified from [34].

1.2.3 Thalamocortical afferents (ocular dominance columns)

When kittens are born, the thalamocortical afferents from the two eyes are overlapping in cortical layer IV, the input layer of primary visual cortex [44]. The segregation of these projections into alternating patches, called ocular dominance columns occurs during early life starting at about 3 weeks of age [44, 45]. A large number of studies has clearly shown that the formation of ocular dominance columns is driven by activity-dependent competition between the thalamocortical afferents of the two eyes whereby the temporal patterning of neural activity conveys the essential information for the axons to segregate [46, 47]: When neuronal activity is completely blocked in the eyes, the patches do not develop. Reduced activity (e.g. by dark-rearing) reduces the degree of segregation whereas the elimination of correlated activity between the eyes, as it occurs in strabismus, enhances segregation. Column formation thus seems to be the result of a competitive self-organizing pro-

cess. Whether similar mechanisms are also responsible for the final expression of the columnar pattern, that is, for the spacing of adjacent columns, their width, and location, is still a matter of debate.

Direct evidence for an activity-dependent development of the pattern of ocular dominance domains was obtained in a study with strabismic cats [34]. In this study, the spacing of adjacent columns in strabismic cats was significantly larger than in normally raised controls (Fig. 7). In agreement with an important role of correlated activity for the determination of columnar spacing, similar observations were reported in monocularly raised cats [48] and in cats with alternating monocular exposure [49]. Furthermore, in a recent longitudinal optical imaging study that followed up the development of columnar patterns in area 17 of kittens before and after induction of a squint angle, an expansion of ocular dominance column spacing of 20% was observed between the 4th and 8th week [50]. However in two recent conference reports [51, 52], columnar spacing was similar in strabismic and normally raised cats. These data are not easy to reconcile with the previous observations. It is possible that the interindividual variability is much larger than previously supposed and that genetic differences might have an influence on columnar spacing or on the susceptibilty for activity related factors. Further experiments are necessary in order to clarify these issues.

2 The dynamics of cortical pattern formation

As described in the preceeding sections, synaptic rearrangement appears to be the basic process driving pattern formation during visual cortical development. Ocular dominance columns segregate as synaptic connections from one eye are elaborated in some cortical regions while retracting from others. Also tangential connections become clustered and selective through elaborating 'appropriate' and retracting 'inappropriate connections'. For both systems evidence suggests that afferent and cortical activity patterns guide the rearrangement of connections such that connections between neurons exhibiting correlated activity patterns are selectively elaborated and stabilized. Modeling studies have demonstrated that similar mechanisms may also induce orientation selectivity in an initially unselective network [24, 25]. At present there is, however, no unambiguous experimental evidence for an activity–dependent self–organization of orientation preference [53, 54].

While pattern formation in the primary visual cortex results from the coordinated rearrangement of about 10^{10} synapses, the emerging structures can be described in relatively simple terms. They consist of repetitive patterns of domains, in which neurons share a common stimulus selectivity or connectivity structure. In analogy to patterns in more simple physical systems like Bénard convection or reaction-diffusion systems, the arrangement of cortical domains may be described by simple order parameter fields. For instance, it appears convenient to describe the pattern of ocular dominance columns by

an abstract order parameter field $o(\mathbf{x})$ where $\mathbf{x}$ denotes the location within the cortical layer and the regions defined by $o(\mathbf{x}) > 0$ and $o(\mathbf{x}) < 0$ represent the left and right eye columns. The emergence of ocular dominance columns during development may then be described by a dynamics of the field $o(\mathbf{x})$. Using such an approach we will analyze the properties and dynamics of cortical patterns in the following sections.

For analyzing the formation of ocular dominance patterns, we will construct a simple model equation, which describes the development of the pattern based on biologically plausible rules for synaptic rearrangement. We will show that this model can be used to understand collective properties of the pattern forming process, such as the wavelength of the emerging structure, the stability or instability of the homogeneous state and the dependence of these properties on visual experience. Assuming that a similar equation describes the development of the pattern of orientation preferences, we will discuss the possibility that the pattern is subject to substantial rearrangement during visual development. Our numerical simulations indicate that the pinwheels in orientation preference maps exhibit a tendency to move and annihilate after the initial emergence of the pattern of orientation columns. We will argue that this behavior can be predicted using only a few, biologically plausible symmetry assumptions.

2.1 Ocular dominance segregation

Our primary aim in this section is the dynamics of the field $o(\mathbf{x})$ which governs the emergence of the pattern of ocular dominance columns from a homogeneous initial state, and in particular its dependence on parameters describing visual experience. Such a dynamics can be derived from a dynamics of synaptic strengths which models basic learning mechanisms. In the following we will first construct a simple, phenomenological synaptic dynamics which is driven by Hebbian modifications and through which the total strength of synapses onto a cortical neuron is stabilized by an activity–dependent dynamic process. Using a set of idealizing assumptions on the shape of cortical activity patterns we will then derive a dynamics for the order parameter field $o(\mathbf{x})$.

In a stabilized Hebbian dynamics, the elementary learning rule for the synaptic strength $W(\mathbf{r}, \mathbf{x})$ that links a neuron at location $\mathbf{r}$ in a model retina to a neuron at location $\mathbf{x}$ in the model cortex is composed of a Hebbian term modeling how synaptic strengths change as a function of correlated pre- and postsynaptic activity and non–Hebbian terms which ensure that a measure of total synaptic strength is conserved. Since all variants of Hebbian rules suffer from the same fundamental instability problem we restrict our attention to the simplest term given by

$$\delta W(\mathbf{r}, \mathbf{x}) \propto [a(\mathbf{r})e(\mathbf{x}) - f(W(\mathbf{r}, \mathbf{x}), e(\mathbf{x}))] \tag{1}$$

where $\delta W(\mathbf{r},\mathbf{x})$ is the modification of synaptic strength induced by an afferent activity pattern $a(\mathbf{r})$ and $e(\mathbf{x})$, the activity pattern that forms as a response to $a(\mathbf{r})$ in the cortical target layer. It is easy to see that the first term considered in isolation is unstable. Since the activities $a(\mathbf{r})$ and $e(\mathbf{x})$ are both positive, synaptic strengths can only increase through the first term and in general will diverge as time proceeds. This implies that additional influences must exist which stabilize the synaptic dynamics. In Eq.(1) we assumed that these influences are synaptically local, i.e. for every individual synaptic connection the stabilizing component $f(\cdot)$ depends only on the instantaneous strength of the synapse $W(\mathbf{r},\mathbf{x})$ and on the postsynaptic activity of the cortical neuron under consideration $e(\mathbf{x})$.

If $W(\mathbf{r},\mathbf{x})$ changes slowly through the cumulative effect of a large number of activity patterns its temporal evolution follows the dynamics

$$\frac{\partial}{\partial t}W(\mathbf{r},\mathbf{x}) = \langle a(\mathbf{r})e(\mathbf{x}) - f(W(\mathbf{r},\mathbf{x}),e(\mathbf{x}))\rangle \tag{2}$$

where t denotes time and $\langle\,\rangle$ represents the average over an ensemble of afferent activity patterns. The simplest dynamics of the form (2) that dynamically leads to the conservation of total synaptic strength is identified by expanding $f(W(\mathbf{r},\mathbf{x}),e(\mathbf{x}))$ in a power series

$$f(W(\mathbf{r},\mathbf{x}),e(\mathbf{x})) = f_0 + f_1^W\, W(\mathbf{r},\mathbf{x}) + f_1^e\, e(\mathbf{x}) + f_2^{We}\, W(\mathbf{r},\mathbf{x})\, e(\mathbf{x}) + \ldots \tag{3}$$

and asking which of the successively more complicated terms is sufficient to stabilize the synaptic dynamics. It is easy to convince oneself that the first three terms cannot stabilize the dynamics. The fourth term however is in itself sufficient to stabilize Eq.(1) and leads to a dynamic regulation of the total synaptic strength. Firstly, with $f(W(\mathbf{r},\mathbf{x}),e(\mathbf{x})) = f_2^{We}\, W(\mathbf{r},\mathbf{x})\, e(\mathbf{x})$ the synaptic strength $W(\mathbf{r},\mathbf{x})$ cannot leave the region defined by $0 \leq W(\mathbf{r},\mathbf{x}) < a_{max}/f_2^{We}$ where a_{max} is the maximal activity value in the ensemble of afferent activity patterns. Secondly, the total afferent synaptic strength converging onto a cortical neuron $w_{tot}(\mathbf{x}) = \int d^2r\, W(\mathbf{r},\mathbf{x})$ develops according to the equation

$$\frac{\partial}{\partial t}w_{tot}(\mathbf{x}) = \left\langle \int d^2r\, a(\mathbf{r})\, e(\mathbf{x}) - f_2^{We}\, e(\mathbf{x})\, w_{tot}(\mathbf{x}) \right\rangle \tag{4}$$

and therefore converges towards

$$w_{tot}^{\infty}(\mathbf{x}) = \frac{\langle e(\mathbf{x}) \int d^2r\, a(\mathbf{r})\rangle}{f_2^{We}\, \langle e(\mathbf{x})\rangle} \tag{5}$$

when the dynamics (2) settles into a stationary state. Assuming the total afferent activity $\int d^2r\, a(\mathbf{r})$ to be constant in the ensemble of afferent activity patterns, Eq.(5) implies that the total synaptic strength converges to the same value $\int d^2r\, a(\mathbf{r})/f_2^{We}$ for every cortical neuron. Even if afferent activity

patterns differ in their total activity $w_{tot}(\mathbf{x})$ will in general assume a well defined equilibrium value for every cortical neuron.

The simplest stabilized Hebbian dynamics therefore takes the form

$$\frac{\partial}{\partial t} W(\mathbf{r}, \mathbf{x}) = \langle a(\mathbf{r})\, e(\mathbf{x}) - W(\mathbf{r}, \mathbf{x})\, e(\mathbf{x}) \rangle \tag{6}$$

where f_2^{We} is set to unity without loss of generality. Eq.(6) represents a generalization of models previously called competitive–Hebbian models (see [55, 56]). The dynamic normalization of total synaptic strength in such models was first pointed out by Ritter [57].

In order to model ocular dominance segregation we must consider connections $W_L(\mathbf{r_L}, \mathbf{x})$ and $W_R(\mathbf{r_R}, \mathbf{x})$ from the left and the right eye, respectively. The order parameter $o(\mathbf{x})$ describing the pattern of ocular dominance columns can be defined in terms of these connections as

$$o(\mathbf{x}) = \int d^2r \, (W_L(\mathbf{r}, \mathbf{x}) - W_R(\mathbf{r}, \mathbf{x})) \tag{7}$$

where we assume a common coordinate system in the two retinae. Eq.(6) then implies a dynamics for the field $o(\mathbf{x})$ itself

$$\begin{aligned} \frac{\partial}{\partial t} o(\mathbf{x}) &= \left\langle \left(\int d^2r (a_L(\mathbf{r}) - a_R(\mathbf{r})) - \int d^2r (W_L(\mathbf{r}, \mathbf{x}) - W_R(\mathbf{r}, \mathbf{x})) \right) e(\mathbf{x}) \right\rangle \\ &= \langle (s - o(\mathbf{x}))\, e(\mathbf{x}) \rangle \end{aligned} \tag{8}$$

where the activity patterns $a_L(\mathbf{r})$ and $a_R(\mathbf{r})$ in the left and right retina define a formal ocular dominance stimulus $s = \int d^2r (a_L(\mathbf{r}) - a_R(\mathbf{r}))$.

To complete the definition of the model we must finally specify the cortical activity pattern $e(\mathbf{x})$ in response to an individual afferent stimulus. Here we assume that the activity pattern $e(\mathbf{x})$ is dominantly shaped by interactions within the cortical layer. If neighboring units in the cortical layer are linked such that excitation spreads locally within the layer then cortical activity patterns will be composed of domains of locally coactivated neurons. As a mathematical idealization of this behavior we assume, following Kohonen [58], that the cortical activity pattern is given by a stereotyped activity blob

$$e(\mathbf{x}) = \frac{1}{2\pi\sigma^2} \exp\left(-\frac{|\mathbf{x} - \mathbf{x}^*|^2}{2\sigma^2} \right) \tag{9}$$

where $\mathbf{x}^*$ is the position of the most activated neuron $\mathbf{x}^*$ and σ measures the size of a coactivated cortical domain (CCD). Given this idealization, afferent stimuli determine only the position $\mathbf{x}^*$ of the CCD but not its shape and size. The location of the CCD is therefore a functional of the stimulus and of the present synaptic strengths $\mathbf{x}^* = \mathbf{x}^*(a_L(\cdot), a_R(\cdot), W_L(\cdot)), W_R(\cdot))$.

Assuming a single activated domain, like in Eq.(9), is justified if we restrict the afferent activity patterns $a_L(\cdot), a_R(\cdot)$ to be localized in retinal coordinates.

The activity center $\mathbf{x}^*$ will then be located in the vicinity of the position, which retinotopically corresponds to the center

$$\mathbf{r}_s = \frac{\int d^2r\, \mathbf{r}\, (a_L(\mathbf{r}) + a_R(\mathbf{r}))}{\int d^2r\, (a_L(\mathbf{r}) + a_R(\mathbf{r}))} \tag{10}$$

of the afferent stimulus. In the following, we assume that the retinotopic organization is isotropic, homogeneous, and identical, i.e. that

$$\mathbf{R}_L(\mathbf{x}) = \mathbf{R}_R(\mathbf{x}) = \mathbf{x} \tag{11}$$

with $\mathbf{R}_L(\mathbf{x}) = \int d^2r\, \mathbf{r}\, W_L(\mathbf{r}, \mathbf{x})$ and $\mathbf{R}_R(\mathbf{x}) = \int d^2r\, \mathbf{r}\, W_R(\mathbf{r}, \mathbf{x})$ denoting the receptive field center positions.

In order to keep the model simple our aim is to identify a plausible choice of $\mathbf{x}^*(a_L(\cdot), a_R(\cdot), o(\cdot))$ that leads to a closed form of the dynamics (8) and is capable of describing the development of a pattern of ocular dominance columns. We consider an ensemble of stimuli with variable parameters s localized at variable locations $\mathbf{r}_s$ in the retinae. With the simplest choice $\mathbf{x}^* = \mathbf{r}_s$ the dynamics (8) reduces to

$$\frac{\partial}{\partial t} o(\mathbf{x}) = \langle s \rangle - o(\mathbf{x}) \tag{12}$$

and a pattern of ocular dominance columns cannot form. In general, however, the emerging pattern of ocular dominance columns will modify the position of the activity center $\mathbf{x}^*$. A generalization of $\mathbf{x}^* = \mathbf{r}_s$ is given by

$$\mathbf{x}^* = argmin(|s - o(\mathbf{x})|^2 + |\mathbf{r} - \mathbf{x}|^2) \tag{13}$$

through which the activity center $\mathbf{x}^*$ is shifted towards the neighboring column dominated by the eye which is currently more active.

The model defined by Eqs.(8,9,13) has a homogeneous stationary solution $o_0(\mathbf{x}) = \langle s \rangle$ which in the presence of left - right eye symmetry reduces to $o_0(\mathbf{x}) = 0$. In the following, we will show that the stability of this solution depends on the statistical structure of the afferent activity–patterns and on the size σ of CCDs.

To determine this stability we linearize the dynamics of $o(\mathbf{x})$ in the vicinity of the homogeneous solution. Because the resulting linear equation must be translation invariant in the cortical layer its eigenfunctions will be plane waves. It therefore suffices to study the stability of the model in one spatial dimension

$$\frac{\partial}{\partial t} o(x) = \frac{1}{2\pi\sigma^2} \left\langle (s - o(x)) \exp(-\frac{|x - x^*(s, r, o(\cdot))|^2}{2\sigma^2}) \right\rangle \tag{14}$$

$$= \frac{1}{2\pi\sigma^2} \int ds dr P(s, r)(s - o(x)) \exp(-\frac{|x - x^*(s, r, o(\cdot))|^2}{2\sigma^2}) \tag{15}$$

where $P(s, r)$ is the probability density of stimuli. For simplicity we further assume $P(s, r)$ to be independent of the retinal position $P(s, r) = P(s)$.

The right hand side of the integro–differential equation (13) can be linearized by linearizing the integrand and yields

$$\frac{\partial}{\partial t}\hat{o}(x) = -\hat{o}(x) + \frac{\langle p^2 \rangle}{2\pi\sigma^2} \int dy\ \hat{o}_{xx}(y)\ \exp(-\frac{|x-y|^2}{2\pi\sigma^2}) \tag{16}$$

after performing the p integration. Here $\hat{o}(x) = o(x) - \langle s \rangle$ and $\langle p^2 \rangle = \langle (s - \langle s \rangle)^2 \rangle$. The growth rates of $\hat{o}(x)$, i.e. the eigenvalues of the rhs operator are

$$\lambda(k) = -1 + \langle p^2 \rangle\, k^2 \exp\left(-\frac{k^2\sigma^2}{2}\right) \quad . \tag{17}$$

The maximal eigenvalue belongs to $k_{max} = \sqrt{2}/\sigma$ and is positive for

$$\sigma < \sigma^* = \sqrt{\frac{2\langle p^2 \rangle}{e}} \quad . \tag{18}$$

As a consequence, the homogeneous solution $o_0(x)$ looses stability when the size of CCDs is below the threshold value σ^*. This leads to the emergence of an ocular dominance pattern with characteristic wavelength

$$\Lambda = \sqrt{2}\pi\sigma. \tag{19}$$

One should note that according to this result the same microscopic rules of synaptic plasticity can either lead to the emergence of ocular dominance columns or suppress ocular dominance segregation depending on the size of CCDs.

2.2 Experience–dependence of the pattern wavelength

The above analysis shows that different afferent patterns of activity can influence the emergence of ocular dominance columns only through the instability threshold $\sigma^* = \sqrt{2\langle p^2 \rangle / e}$. Once σ^* is given the dynamics of ocular dominance segregation from a homogeneous initial state is defined. To show that this influence can in fact explain the observed wavelength change we rewrite the instability threshold in terms of the correlation functions

$$\begin{aligned} C_L(q) &= \langle a_L(r)\, a_L(r+q) \rangle - \langle a_L(r) \rangle^2 \\ C_R(q) &= \langle a_R(r)\, a_R(r+q) \rangle - \langle a_R(r) \rangle^2 \\ C_{LR}(q) &= \langle a_L(r)\, a_R(r+q) \rangle - \langle a_L(r) \rangle \langle a_R(r) \rangle \end{aligned} \tag{20}$$

of the afferent activity patterns. Here we assume that the ensemble of activity patterns in both eyes is statistically translation invariant. The expression for the instability threshold is implied by the identity

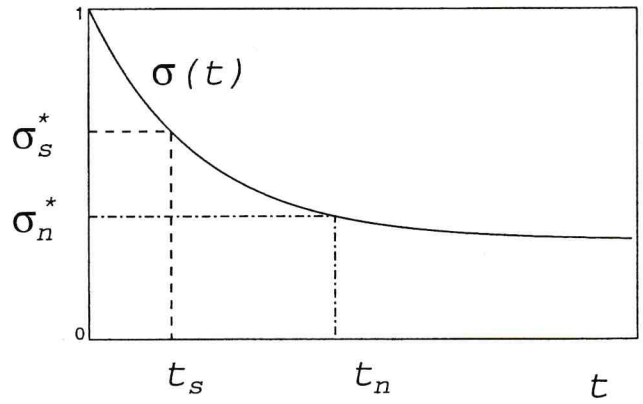

Fig. 8. Relation between visual experience, developmental timing, and pattern wavelength in ocular dominance segregation. The solid line represents the size of coactivated domains as a function of time during development (schematic). Dashed and dash–dotted lines mark the level of σ_s^* and σ_n^* and the corresponding points in time at which the segregation of ocular dominance columns starts, respectively. If σ decreases during development the critical size σ^* determines timing and wavelength of ocular dominance segregation. A larger value of σ^* with squint then leads to an earlier segregation of more widely spaced columns.

$$\begin{aligned}\langle p^2 \rangle &= \left\langle \left(\int d^2 r a_L(r) - \langle a_L(r) \rangle - (a_R(r) - \langle a_R(r) \rangle) \right)^2 \right\rangle \\ &= \int d^2 q \, C_L(q) + C_R(q) - 2C_{LR}(q)\end{aligned}$$

where the area $\int d^2 r$ of the retinae is 1.

This identity determines the dependence of the instability threshold

$$\sigma^* = \sqrt{\frac{2}{e} \int d^2 q \, C_L(q) + C_R(q) - 2C_{LR}(q)} \tag{21}$$

on the statistics of afferent activity patterns.

Squint strongly reduces correlations between activity in the two eyes ($C_{LR} \approx 0$) but leaves the correlations within an eye similar to normal vision. Because $\int d^2 q \, C_L(q) + C_R(q) > 0$ and inter-eye correlations are presumably positive [23] the instability threshold will in general be larger in squinters

$$\sigma^*_{sq} > \sigma^*_{norm} \tag{22}$$

compared to normal animals. In contrast, monocular deprivation reduces not only the inter-eye correlations but also the activity and as a consequence the

correlations in the deprived eye. Therefore

$$\sigma^*_{sq} > \sigma^*_{MD} \tag{23}$$

while the ordering of σ^*_{MD} and σ^*_{norm} depends on details of the correlation functions and no general statements can be made.

If we suppose that the size of CCDs decreases during development it is easy to see that the dependence of the instability threshold on inter-eye correlations leads to more widely spaced columns in squinting animals. Since ocular dominance columns in cats with normal visual experience segregate only several weeks after eye opening σ must be assumed to decrease from a value initially larger than σ^*_{norm}. In this case, σ will reach the threshold $\sigma^*_{sq} > \sigma^*_{norm}$ earlier in squinters than in normal animals. Because the wavelength Λ is proportional to σ when the homogeneous solution becomes unstable this will in turn cause the emergence of ODCs with a larger wavelength (Fig. 8).

2.3 Dynamics of orientation pinwheels

The pinwheel-like arrangement of orientation columns around orientation centers is a ubiquitous structural element of orientation preference maps in primary visual cortex (see section 2). It has long been hypothesized that the pattern of orientation columns arises via activity–dependent refinement of cortical circuitry during early life [24, 59]. Presently there is, however, no direct experimental evidence confirming this hypothesis [60, 61, 42]. In this section, we will discuss possible signatures of an activity–dependent generation of orientation preference during normal development. We will consider the proliferation and dynamics of pinwheels in models of the activity–dependent formation of orientation columns. First we shall outline a probabilistic picture of the emergence of patterns of orientation preferences. Within this picture, symmetry assumptions imply that a minimal density of pinwheels must emerge when orientation selectivity is first established. We shall then argue that this treatment mathematically accurately represents the dynamics of a large class of models for the activity–dependent development of orientation selectivity. The dynamics of pinwheels in this class of models is therefore highly constrained by symmetry principles and predicts distinct, robust, and experimentally verifiable signatures of an activity–dependent generation of orientation preferences.

In analogy to the model for the development of ocular dominance columns constructed above we will assume that the development of the pattern of orientation columns is described by a dynamics

$$\frac{\partial}{\partial t} z(\mathbf{x}) = \mathbf{F}[\mathbf{z}(\cdot)] + \xi\,, \tag{24}$$

of a order parameter field $z(\mathbf{x}) = |\mathbf{z}(\mathbf{x})|\mathrm{e}^{2\mathrm{i}\vartheta(\mathbf{x})}$. The field $z(\mathbf{x})$ is complex valued and $\mathbf{x}$ denotes the location of a column parallel to the cortical surface.

$\vartheta(\mathbf{x})$ denotes its preferred orientation, and $|z(\mathbf{x})|$ measures the orientation selectivity of the average response of neurons within the column. Because different neurons in the center of a pinwheel exhibit the whole range of possible orientation preferences [62] their average response is unselective and $|z(\mathbf{x})|$ vanishes at these locations. Pinwheel centers are therefore the zeros of $z(\mathbf{x})$.

The expected density of pinwheels early in development has been estimated within a probabilistic framework [63]. This estimate is based on the assumption that, if orientation preference emerges by the activity–dependent refinement of initially crude patterns of synaptic connections, then random influences – like (1) a random setup of the initial pattern of connections or (2) an unpredictable sequence of activity patterns that guides the refinement of synaptic connections – determine the emerging pattern of orientation preferences. Mathematically, this assumption is equivalent to considering the emerging pattern of orientation columns as a realization drawn at random from an ensemble of possible patterns. The formation of a pinwheel is then a joint event: If a given column develops at random a preference for e.g. horizontally oriented stimuli, this will happen with a defined probability. There is also a joint probability that at the same time neighboring columns develop preferences for vertical and the two oblique orientations. The overall result of this event is the formation of a pinwheel. How frequently such a configuration is expected to arise in a given area determines the spatial density of pinwheels in the emerging pattern. In order to calculate this density, spatial correlations in the emerging pattern of orientation columns must be taken into account. The emerging orientation preferences of nearby columns must be highly correlated because orientation preferences change continuously across the cortex as soon as the pattern can be visualized experimentally (around the time of eye–opening) [64]. Furthermore separate orientation columns of the same orientation preference exhibit a typical spacing Λ early on [64]. Considered statistically, this implies that the orientation preferences that emerge in columns, which are one Λ apart, must be positively correlated. In order to calculate the expected density of pinwheels ρ one may assume that these correlations - whatever their exact form - depend only on the distance between columns and completely specify the ensemble. The emerging pattern then realizes a homogenous and isotropic Gaussian random field and the expected density of pinwheels is given by

$$\rho = \frac{\pi}{\Lambda^2} \, (1 + \alpha) \tag{25}$$

where α is a number that describes the structure of spatial correlations [63]. α vanishes if patterns exhibit only a vanishingly small range of wavelengths and is positive if a finite range is present. Eq.(25) therefore implies that one expects to find on average at least $\pi \simeq 3.1$ pinwheels in an area of size Λ^2. In [63] two assumptions were used to derive Eq.(25):

(1) Two-point correlations in the emerging pattern depend only on the distance between columns.

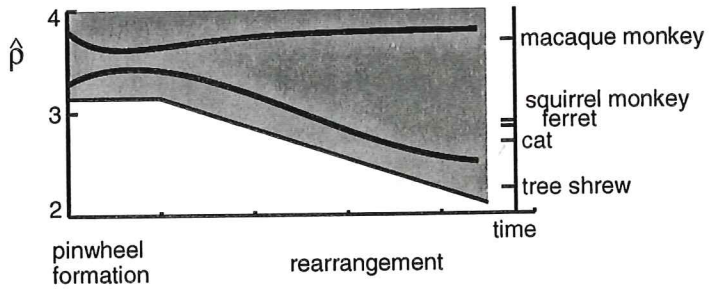

Fig. 9. Activity–dependent mechanisms constrain the scaled density of pinwheels during development. Shaded area: accessible range for allowed trajectories of $\hat{\rho}(t) = \rho A^2$ as a function of time (x-axis) during development according to Eqs.(24,25). Two possible trajectories are displayed (lines). Right axis: observed scaled pinwheel densities in adult animals of different species (see [63]). Low densities as observed e.g. in cats and tree shrews can only develop through an initial overproduction and subsequent annihilation of pinwheels. Reproduced from [63] with the permission of *Nature*.

(2) Gaussian statistics: These correlations are sufficient to specify the ensemble of possible early patterns.

Assumption (1) is related to a set of symmetries. It is correct if, given that one particular pattern of orientation columns can emerge, the patterns that result from

(a) shifting the pattern parallel to the cortical surface or

(b) rotating the pattern parallel to the cortical surface or from

(c) shifting all orientation preferences by the same angle

in principle may form as well and will arise with the same probability. Assumption (2) implicates the notion that a large number of random factors determine the pattern of orientation columns (central limit theorem). Qualitatively this appears very plausible: The elementary event in any model of activity–dependent development is the modification of neuronal selectivities by a pattern of neuronal activity. In the visual cortex, orientation selectivity arises over a period of many hours or a few days [65, 64]. The activity patterns which drive this process are presumably only correlated over time intervals in the order of seconds. Therefore the pattern must in fact arise through the cumulative effect of a large number of independent activity patterns which individually might induce only minor changes.

Any model of visual cortical development that obeys assumptions (1) and (2) will produce a density of pinwheels in accord with Eq.(25). In particular, the very general class of models defined by a dynamics like Eq.(24) and the group of symmetries (a)-(c), if beginning from random initial conditions,

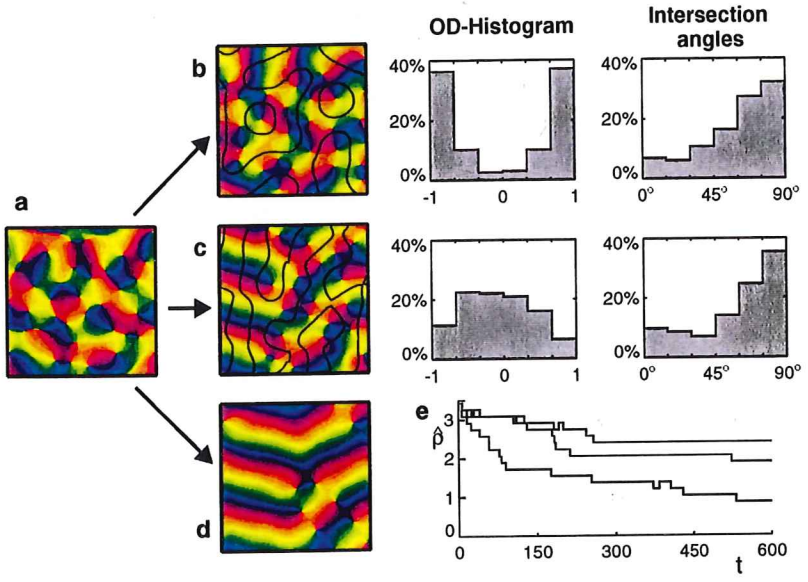

obeys these assumptions during the initial organization of an orientation pattern [63]. Therefore any such model must produce initial patterns with a pinwheel density of $\rho \geq \pi/\Lambda^2$. How an individual pattern transforms according to Eq.(24) depends on the precise form of the dynamics and therefore on the specific rules governing activity–induced changes. However, the kind of patterns that emerge when orientation selectivity is first established from a random unselective initial state is common to all models that exhibit the symmetries (a)-(c).

2.4 Pinwheel movement during development

It is not implied that lower densities of pinwheels cannot develop within this class of models. However, densities $\rho < \pi/\Lambda^2$ are predicted to form from an early high density state through a secondary reduction of the number of pinwheels. The only way to reduce the number of pinwheels by continuously rearranging the pattern is the collision and annihilation of pairs of pinwheels with opposite chirality [66]. The considered class of models therefore also predicts that pinwheel densities $\rho < \pi/\Lambda^2$, if found, have been formed through the motion and annihilation of pinwheels (Fig. 9).

Low pinwheel densities have indeed been observed in adult animals (see Fig. 9). In Figure 9 the scaled pinwheel density $\hat{\rho} = \rho\Lambda^2$ in five different species is displayed. The abundance of pinwheels clearly varies across species.

Fig. 10. Rearrangement of an orientation map in the presence or absence of ocular dominance columns. (**a**) early and late (**b-d**) patterns of orientation columns and ocular dominance borders (black lines) in three simulations of the elastic network [68, 55] (for methods see [67]) started from the same initial pattern ((**a**) $t = 10$) but with different degrees of ocular dominance segregation: (**b**) strong ocular dominance segregation (most units are monocular), (**c**) intermediate ocular dominance segregation (most units are binocular), and (**d**) no ocular dominance segregation (all at $t = 600$). Color code as in Figure 5. The graphs to the right of (**b**) and (**c**) show the ocular dominance histogram (left) and the histogram of intersection angles between ocular dominance borders and iso–orientation domains (right) for the patterns in (**b**) and (**c**), respectively. Ocular dominance borders impose a geometric constraint on the pattern of orientation columns. In both patterns (**b**) and (**c**), iso–orientation domains exhibit a tendency to intersect ocular dominance borders at steep angles: steep intersection angles ($\psi \approx 90$ deg) are more frequent that shallow angles ($\psi \approx 0$ deg). The simulations show that this constraint impairs pinwheel annihilation more strongly with stronger ocular dominance segregation. The ocular dominance histograms show the frequencies of different ocular dominance values o. Ocular dominance values o are binned into 6 equidistant classes. Units that prefer one eye ($o \approx \pm 1$) are most frequent in (**b**). Units that are binocular ($o \approx 0$) are most frequent in (**c**). (**e**) The scaled density of preserved pinwheels $\hat{\rho}$ increases with the degree of ocular dominance segregation. $\hat{\rho}(t)$ for the three simulations (top: strong ocular dominance segregation; middle: intermediate ocular dominance segregation; bottom: no ocular dominance columns). Steps in (**e**) represent individual annihilation (and occasionally production) events. Reproduced from [63] with the permission of *Nature*.

Macaque monkeys exhibit the largest and tree shrews the smallest scaled pinwheel densities while squirrel monkeys, ferrets, and cats show intermediate values. Theoretically, scaled densities $\hat{\rho} < \pi$ imply pinwheel–annihilation during development (Fig. 9). Pinwheel–annihilation is therefore predicted to occur in cat and tree shrew striate cortex. Pinwheel–annihilation may also occur in ferrets and squirrel monkeys. It may not occur in macaque monkeys. Furthermore the data suggest a relation between ocular dominance segregation and pinwheel density. Species in which pronounced ocular dominance columns are present (such as macaque monkeys) exhibit a higher scaled density compared to species in which ocular dominance columns are weak or absent (i.e. tree shrews).

Since pinwheel–annihilation is predicted to occur in several species the question arises of whether pinwheels do typically move in concrete models of visual development. Their dynamics has therefore been investigated in several biologically plausible models [63, 67]. Figure 10 shows results from one of them proposed originally by Durbin and Mitchinson [68]. It is assumed in this model that the orientation preferences of cortical units change in response to afferent stimuli, which are described by their location and orientation in visual field coordinates. Cortical units are activated if their

receptive field position and orientation preference are close to the stimulus. Units unselective for stimulus orientation are activated if a stimulus is close to their receptive field position. The selectivities of activated units are then changed to better match the stimulus. At the same time, neighboring units interact such that the smoothness of selectivities across the cortical layer is enhanced. When starting from an initial condition in which all cortical units are not orientation selective, application of the same rules can induce the formation of a pattern of orientation columns. By assigning cortical units an ocular dominance index and introducing stimuli which are either binocular or dominated by one eye, this model has been generalized to describe the coordinated development of orientation and ocular dominance columns [55]. In this case, stimuli are assumed to activate those units more strongly whose ocular dominance matches the stimulus' dominant eye. Analogous to the treatment of orientation preferences, the ocular dominance of activated neurons is then changed towards the eye which dominates the stimulus.

In agreement with the theory outlined above, more than π/A^2 pinwheels proliferate as a pattern of orientation columns arises from an initially unselective state (Fig. 10a,e). This early pattern is not stable but rearranges under the influence of continuing stimulus–driven changes. The predominant process during this rearrangement is the motion, collision, and annihilation of pairs of pinwheels. In Figure 10 three simulations starting from the same early orientation map are compared. These simulations utilize sets of stimuli that lead to strong (Fig. 10b), intermediate (Fig.10c), or no ocular dominance segregation (Fig. 10d). The speed and degree of pinwheel–annihilation in these simulations reflects the degree of ocular dominance segregation (Fig. 10e). The number of annihilating pinwheel pairs is largest without ocular dominance segregation (Fig. 10b), smaller with an intermediate degree of ocular dominance segregation (Fig. 10c), and least with strong ocular dominance segregation (Fig. 10b). In a large number of similar simulations, it was observed that (1) the tendency of pinwheels to annihilate after the initial emergence of orientation selectivity and (2) the ability of ocular dominance segregation to slow down or stop pinwheel–annihilation were independent of model parameters and details [67]. A simple explanation of the observed interspecies differences in the scaled pinwheel density therefore is that species in which ocular dominance columns are weak or absent perform extensive pinwheel–annihilation while strong ocular dominance segregation prevents a reduction of the pinwheel density during development. In conclusion, these results indicate that an activity–dependent origin of preference has robust and distinct signatures in the dynamics of pinwheels during development. Verification of the prediction that pinwheels move and annihilate in species that exhibit low densities of pinwheels in the adult would indeed provide strong evidence for an activity–dependent generation of orientation preferences in the visual cortex.

3 Conclusions

Pattern formation in the developing visual cortex is a complex process that involves a multitude of interactions at the molecular, cellular, and network level. Considered phenomenologically at the level of cortical domains this process shares many characteristics with pattern formation in more simple physical systems. We have presented a few examples of a mathematical analysis of cortical pattern formation problems inspired by this analogy. Our results stress the importance of the interactions among cortical neurons in shaping the functional architecture of the visual cortex during development: In the brain, intracortical and afferent connections develop in parallel. In mathematical models of cortical development, intracortical interactions shape the dependence of the patterns' properties on visual experience and lead to the dynamic rearrangement of cortical columns that is predicted to occur during development. Understanding the impact of these interactions on the process of 'learning to see' will require a close coordination of theoretical and experimental efforts.

References

1. Purves, D., Augustine, G., Fitzpatrick, D., Katz, L., LaMantia, A.-S., and McNamara, J. *Neuroscience.* Sinauer, Sunderland, MA, (1997).
2. Hubel, D. H. *Auge und Gehirn: Neurobiologie des Sehens.* Spektrum-der-Wissenschaft-Verlagsgesellschaft, Heidelberg, (1989).
3. Buser, P. and Imbert, M. *Vision.* MIT Press, Cambridge, MA, (1992).
4. Hubel, D. H. and Wiesel, T. N. *J. Physiol.* **160**, 215–243 (1962).
5. Sompolinsky, H. and Shapley, R. *Current Opinion in Neurobiology* **7**, 514–522 (1997).
6. Gilbert, C. *Neuron* **9**, 1–13 (1992).
7. Löwel, S. and Singer, W. In *Perceptual Learning*, Fahle, M. and Poggio T., editors (MIT-Press, Cambridge MA, 1999).
8. Sokoloff, L. *Int. Rev. Neurobiol.* **22**, 287–333 (1981).
9. Grinvald, A., Lieke, E., Frostig, R., Gilbert, C., and Wiesel, T. *Nature* **324**, 361–364 (1986).
10. Toga, A. W. and Mazziota, J. C. *Brain Mapping : The Methods.* Acad. Press, San Diego, (1996).
11. Bonhoeffer, T. and Grinvald, A. *Nature* **353**, 429–431 (1991).
12. Blasdel, G. G. and Salama, G. *Nature* **321**, 579–585 (1986).
13. Bonhoeffer, T., Kim, D.-S., Malonek, D., Shoham, D., and Grinvald, A. *Eur. J. Neurosci.* **7**, 1973–1988 (1995).
14. Bartfeld, E. and Grinvald, A. *Proc. Natl. Acad. Sci.* **89**, 11905–11909 (1992).
15. Blasdel, G. G. *J. Neurosci.* **12**, 3139–3161 (1992).
16. Blasdel, G. G., Livingstone, M., and Hubel, D. *Soc. Neurosci. Abstracts* 12, 1500 (1993).
17. Weliky, M. and Katz, L. C. *J. Neurosci.* **14**, 7291–7305 (1994).
18. Rao, S., Toth, L., and Sur, M. *J. Comp. Neurol.* **387**, 358–370 (1997).

19. Bosking, W. H., Zhang, Y., Schofield, B. R., and Fitzpatrick, D. *J. Neurosci.* **17**, 2112–2127 (1997).
20. Hebb, D. O. *The Organization of Behavior.* John Wiley and Sons, NY, (1949).
21. Hubel, D. H. and Wiesel, T. N. *J. Neurophysiol.* **28**, 1041–1059 (1965).
22. Stent, G. S. *Proc. Nat. Acad. Sci. USA* **70**, 997–1001 (1973).
23. Miller, K. D., Keller, J., and Stryker, M. *Science* **245**, 605–615 (1989).
24. von der Malsburg, C. *Kybernetik* **14**, 85–100 (1973).
25. Miller, K. D. *J. Neurosci.* **14**, 409–441 (1994).
26. Katz, L. C. and Callaway, E. M. *Ann. Rev. Neurosci.* **15**, 31–56 (1992).
27. Wiesel, T. N. *Nature* **299**, 583–591 (1982).
28. Löwel, S. and Singer, W. *Science* **255**, 209–212 (1992).
29. Sokoloff, L., Reivich, M., Kennedy, C., Rosiers, M. D., Patlak, C., Pettigrew, K., Sakurada, O., and Shinohara, M. *J. Neurochem.* **28**, 897–916 (1977).
30. Gilbert, C. and Wiesel, T. *J. Neurosci.* **9**, 2432–2442 (1989).
31. Schmidt, K., Kim, D., Singer, W., Bonhoeffer, T., and Löwel, S. *J. Neurosci.* **17**, 5480–5492 (1997).
32. Löwel, S., Schmidt, K., Kim, D., Wolf, F., Hoffsümmer, F., Singer, W., and Bonhoeffer, T. *Eur. J. Neurosci.* **10**, 2629–2643 (1998).
33. Crair, M., Gillespie, D., and Stryker, M. *Science* **279**, 566–570 (1998).
34. Löwel, S. *J. Neurosci.* **14**, 7451–7468 (1994).
35. Obermayer, K. and Blasdel, G. G. *J. Neurosci.* **13**, 4114–4129 (1993).
36. Hübener, M., Shoham, D., Grinvald, A., and Bonhoeffer, T. *J. Neurosci.* **17**, 9270–9284 (1997).
37. Crair, M., Ruthazer, E., Gillespie, D., and Stryker, M. *Neuron* **19**, 307–318 (1997).
38. Hubel, D. H. and Wiesel, T. N. *Proc. Royal Soc. London (Biol.)* **198**, 1–59 (1977).
39. Swindale, N. *Biol. Cybern.* **65**, 415–424 (1991).
40. Hubel, D. H. and Wiesel, T. N. *J. Neurophysiol.* **26**, 994–1002 (1963).
41. Mioche, L. and Singer, W. *J. Neurophysiol.* **62**, 185–197 (1989).
42. Gödecke, I. and Bonhoeffer, T. *Nature* **379**, 251–254 (1996).
43. Kim, D.-S. and Bonhoeffer, T. *Nature* **370**, 370–372 (1994).
44. LeVay, S., Stryker, M. P., and Shatz, C. *J. Comp. Neurol.* **179**, 223–244 (1978).
45. Shatz, C. J. and Stryker, M. P. *J. Physiol. (London)* **281**, 267–283 (1978).
46. Stryker, M. P. In *Development of the Visual System,* Lam, D. M. and Shatz, C. J., editors, volume 3 of *Proceedings of the Retina Resarch Foundation Symposia*, chapter 16, 267–287. MIT Press, Cambridge, Mass (1991).
47. Goodman, C. S. and Shatz, C. J. *Neuron* **10**, 77–98 (1993).
48. Schmidt, K. and Löwel, S. In *Sensorische Transduktion*Elsner, N. and Breer, H., editors, 501, (1994).
49. Tieman, S. and Tumosa, N. *Visual Neurosci.* **14**, 929–938 (1997).
50. Sengpiel, F., Gödecke, I., Stawinski, P., Hübener, M., Löwel, S., and Bonhoeffer, T. *Neuropharmacology* **37**, 607–621 (1998).
51. Jones, D., Murphy, K., and Sluyters, R. V. *Inv.Ophthalmol.Vis.Sci.*, 37, 1964, (1996).
52. Rathjen, S., Schmidt, K., and Löwel, S. *Göttinger Konferenz der Neurowissenschaftlichen Gesellschaft*, (1999).

53. Wolf, F., Bauer, H.-U., Pawelzik, K., and Geisel, T. *Nature* **382**, 306–307 (1996).
54. Hübener, M. *Current Biology* **8**, R342–R345 (1998).
55. Erwin, E., Obermayer, K., and Schulten, K. *Neural Comp.* **7**, 425–468 (1995).
56. Swindale, N. *Network* **7**, 161–247 (1996).
57. Ritter, H. and Schulten, K. *Biol. Cybern.* **54**, 99–106 (1986).
58. Kohonen, T. *Biol. Cybern.* **43**, 59–69 (1982).
59. Nass, M. M. and Cooper, L. N. *Biol. Cybern.* **19**, 1–18 (1975).
60. Movshon, J. and Sluyters, R. C. V. *Ann. Rev. Psychol.* **32**, 447–522 (1981).
61. Frégnac, Y. and Imbert, M. *Physiological Reviews* **64**(1), 325–434 (1984).
62. Maldonado, P. E., Gödecke, I., Gray, C. M., and Bonhoeffer, T. *Science* **276**, 1551–1555 (1997).
63. Wolf, F. and Geisel, T. *Nature* **395**, 73–78 (1998).
64. Chapman, B., Stryker, M. P., and Bonhoeffer, T. *J. Neurosci.* **16**, 6443–6453 (1996).
65. Chapman, B. and Stryker, M. P. *J. Neurosci.* **13**, 5251–5262 (1993).
66. Halperin, B. I. In *Physics of Defects, Les Houches, Session XXXV, 1980,* Balian, R., Kléman, M., and Poirier, J.-P., editors (North–Holland, Amsterdam, 1981).
67. Wolf, F. and Geisel, T. *Nature* **395**, http://www.nature.com/supplement (1998).
68. Durbin, R. and Mitchinson, G. *Nature* **343**, 644–647 (1990).